IEEE Access
Multidisciplinary | Rapid Review | Open Access Journal

Received September 25, 2020, accepted September 27, 2020, date of publication September 30, 2020,
date of current version October 9, 2020.

Digital Object Identifier 10.1109/ACCESS.2020.3027891

Heterogeneity-Aware Energy Saving and Energy Efficiency Optimization in Dense Small Cell Networks

SHIE WU[1], RUI YIN[2], (Senior Member, IEEE), AND CELIMUGE WU[3], (Senior Member, IEEE)

[1]School of Opto-Electronic Information Science and Technology, Yantai University, Yantai 264005, China
[2]School of Information and Electrical Engineering, Zhejiang University City College, Hangzhou 310015, China
[3]Graduate School of Informatics and Engineering, The University of Electro-Communications, Tokyo 182-8585, Japan

Corresponding author: Shie Wu (wushie@ytu.edu.cn)

This work was supported in part by the National Natural Science Foundation Program of China under Grant 61771429, in part by ROIS NII Open Collaborative Research under Grant 2020-20S0502, and in part by the JSPS KAKENHI under Grant 20H00592.

ABSTRACT In dense small cell networks (DSCNs), small cells are heterogeneous due to the unplanned deployment and various traffic loads, resulting in different energy efficiency (EE) preferences. In this paper, taking into account the heterogeneity of small cells, energy saving (ES) and EE are jointly optimized through subchannel allocation, subframe configuration and power allocation. In order to quantify the effects of small cells' heterogeneous information on EE, an EE preference function is first defined. Then, the joint ES and EE optimization problem is formulated as a multi-objective optimization problem. Due to the coupling of ES and EE, obtaining the solution is non-trivial. Therefore, we propose a heterogeneity-aware ES and EE (HESEE) optimization algorithm, where subchannel allocation is optimized to ensure the fairness of active subframes required by the users in the same small cell base stations (SBSs). Then subframe configuration is conducted via group formation sleep mechanism. Particularly, address the non-concave sum-of-ratios optimization for system EE, the concave-convex procedure (CCCP) method is adopted. Simulation results show that the proposed HESEE algorithm can optimize the SBSs' EEs according to their EE preferences. In addition, the HESEE algorithm can achieve good performance in reducing energy consumption as well as improving the system EE.

INDEX TERMS Dense small cell networks (DSCNs), energy efficiency (EE), energy saving (ES), heterogeneity-aware, fairness.

I. INTRODUCTION

The rapid evolution of various mobile applications has led to the explosive growth of mobile data traffic in wireless networks. As a promising technology, dense small cell networks (DSCNs) composed of massive small cells can satisfy the data requirements. However, the energy consumption is non-negligible due to the increasingly deployed small cell base stations (SBSs). In recent years, green communications have attracted a lot of attention [1]. Meanwhile, energy saving (ES) and energy efficiency (EE) have become two important goals for next generation of mobile communication system [2]. Therefore, it is urgent to enhance EE with limited valuable energy in the DSCNs.

The associate editor coordinating the review of this manuscript and approving it for publication was Wei Wang.

Due to random deployment of small cells and various service requirements of users, small cells are heterogeneous in the DSCNs, resulting in different EE preferences. For instance, when users' data rate demands are large, i.e., the traffic load of a SBS is high, the SBS should strive to meet its users' data rate requirements and pay more attention to its throughput, resulting in low EE preference. Otherwise, the SBS's EE preference is high if its users' data rate demands are easily met [3]. Therefore, it is necessary to consider the heterogeneity of small cells when optimize the system EE in the DSCNs.

A. RELATED WORK

In order to meet the demand of green communications, many researchers have proposed many different methods to reduce

energy consumption or improve the network EE. In [4], the authors provide the most overview of 5G technologies and discuss resource allocation technologies for green communications in the DSCNs.

Since BSs are typically deployed to guarantee the requirements of peak traffic volume, most of time they are underutilized. Therefore, the underutilized BSs are allowed to sleep to effectively reduce energy consumption. In [5], the authors compare random, distance based, and load based distributed sleep modes for delay-tolerant network traffic. However, sleeping for long time would lead to coverage holes and users served by sleeping SBSs should be transferred to neighbor SBSs [6]. On the other hand, the sleep mode also reduces the EE. Therefore, a system throughput based sleep scheme is proposed to reduce power consumption and enhance EE in [7]. In order to avoid the handover problem in the conventional sleep mode, SBSs can serve users in active subframes and sleep in some inactive subframes to save energy. Therefore, the system EE can be improved via subframe configuration and sleeping mode. In [8], the optimal number of active subframes for one macrocell BS (MBS) is deduced. However, the result is not suitable for the DSCNs due to the severe co-tier interference. In fact, since each SBS usually serves several users, the number of active subframes required by a SBS depends on the needs of its users, which is coupled with the subchannel allocation. However, to the best of our knowledge, there is no work concerning the fairness of the required activate subframes between users in the same SBS for energy saving.

Large numbers of researches focus on resource allocation to maximize the network EE, which is defined as the ratio between the total achievable data rate and the total network power consumption. From the type of available resource in wireless communication network, EE-based resource allocation algorithms can be classified into power domain, frequency domain, time domain, spatial domain and multi-domain combination based methods. In power domain, considering users' quality of service (QoS) requirements, the network EE is improved through transmission power spreading in [9]. Frequency domain approaches are always combined with the power domain to enhance the network EE by joint frequency allocation and power allocation [10]–[14]. In time domain, user association and subframe configuration are jointly considered, where the optimal ratio of almost blank subframes (ABSs) is derived in [15]. In spatial domain, reference [16] optimizes beamforming design at both SBSs and MBS. Combining power domain, frequency domain and spatial domain, a weighted network EE maximization problem is optimized while considering the limited backhaul capacity and users' fairness in [17]. In the aforementioned studies, since the network EE is optimized from the perspective of the whole network, it ignores the heterogeneity between the individual EE preferences.

A few studies on heterogeneity-based EE optimization includes weighted EE modeling [3] and cell load coupling model [18]. In [3], the effect of traffic load on EE preference is modeled by weighted EE optimization, but the weights are only random selected constants without any physical meaning. In [18], the authors propose a load-coupled signal to interference plus noise ratio (SINR) model, in which the BS's traffic load is equivalent to the probability of interference to adjacent cells using the same frequency spectrum. Based on this SINR model, references [19] and [20] minimize the network energy consumption. In [21], both the network EE and weighted sum of the individual EEs are analyzed through resource block (RB) and power allocation. However, the EE weights of the individuals are constant, which can not be adjusted adaptively. In our previous work [22], we only consider the the influence of SBSs' load on EE optimization and energy saving scheme is not concerned.

There are also other methods enhancing network EE or saving energy, such as network planning, energy harvesting (EH) and transfer, and hardware improvement [23]. In [24], the SBS density, transmission power, number of users and attached antennas are jointly optimized to maximize EE. In order to reduce on-grid power consumption, a renewable SBS serves users only if it has harvested enough energy in a time slot [25]. However, renewable resources depend heavily on the environment and cannot guarantee a stable energy supply. In wireless environment, simultaneous wireless information and power transfer (SWIPT) technology can provide energy supply to wireless network by using radio frequency signals. In [26], the EE optimization problem for OFDM-based 5G wireless networks with SWIPT is studied. However, accurate information decoding must be carried out while the energy acquisition, which is challenging because of the different sensitivities of wireless information receivers and energy receivers. In [27], high EE power amplifier is designed by reducing peak-to-average power ratio through direct current circuit design, signal processing and coding design. In [28], the authors optimize the locations and utilization of the virtual machine (VM) servers to minimize power consumption. In [29], virtual network functions (VNFs) placement and traffic routing are jointly optimized to improve system EE.

As two main aspects of green communications, EE optimization is carried out by considering the throughput as well as the energy consumption while ES aims to minimize energy consumption only. Although these two goals might seemingly different, they are coupled due to the fact that both of them consider the energy consumption. In particular, minimizing the transmission power can save the energy, but it may degrade the EE. On the other hand, resource allocation for maximizing EE usually cannot guarantee the minimum energy consumption under the QoS constraints. Therefore, how to efficiently utilize the limited wireless resources to obtain optimal EE and ES needs to be further explored [30]. However, the existing studies usually focus on EE optimization and ES separately. In the existing researches on EE optimization, considering the heterogeneity of individuals, the sum of individual EEs is usually optimized by setting the EE weights to be constant in [3] and [21]. However, the correlation between constant EE weights and heterogeneous

information is not clearly quantified. In the existing studies on ES, traditional sleep mode would decrease EE significantly because some SBSs with higher throughput might be switched into sleep mode. In [7], a SBS can sleep only when the system throughput is enhanced when its users hand over to a new SBS. However, the sleep technique is two complex in the DSCN with lots of SBSs and SUEs. Motivated by [8], SBSs sleep in subframes can attain the tradeoff of energy saving and throughput loss. However, since each SBS serves several SUEs with various target data requirements, the number of active subframes for each SBS should be optimized.

B. CONTRIBUTIONS AND ORGANIZATION

To the best of our knowledge, quite few work conducts the researches on the joint ES and EE optimization while considering heterogeneity of small cells. In this paper, considering small cells' heterogeneity and cooperation opportunities, our goal is to consume as little energy as possible to improve the sum of SBSs' EEs through subchannel allocation, subframe configuration and power allocation. Our initial conference paper [31] does not consider the influences of subchannel allocation on subframe configuration and users' various target data rates. Moreover, the group formation process is complicated. In this manuscript, considering different users' rate requirements, we propose fairness-based subchannel allocation and group-based subframe configuration algorithms with low complexity in a more practical scenario, and provide more numerical simulations and analyses. The contributions of this paper are summarized as follows:

1) Existing studies mainly focus on ES or EE optimization. In this paper, we optimize ES and EE simultaneously via subchannel allocation, subframe configuration and power allocation, which is formulated as a multi-objective optimization problem. Then, a heterogeneity-aware optimization algorithm is designed to solve the thorny problem.

2) Considering the heterogeneity of small cells in the DSCN, we analyze the impacts of small cells' heterogeneous information on EE optimization and quantify the effects by an EE preference function. Therefore, the EE preferences of small cells can be adjusted adaptively according to their information.

3) Due to the limited subchannels and the coupling of subchannel allocation and subframe configuration, the ES optimization via subchannel allocation and subframe configuration is difficult to solve. Thus, a fairness-based subchannel allocation algorithm and a group-based subframe configuration algorithm are proposed to deal with the problem.

4) Since the heterogeneity-aware EE maximization problem is a non-concave sum-of-ratios optimization, obtaining the optimal power allocation for EE optimization directly is arduous. However, the Dinkelbach method [32] used in [17] is no longer available. Therefore, we adopt the concave-convex procedure (CCCP) method to address EE maximization problem by transforming it into a difference-of-convex formation in this paper.

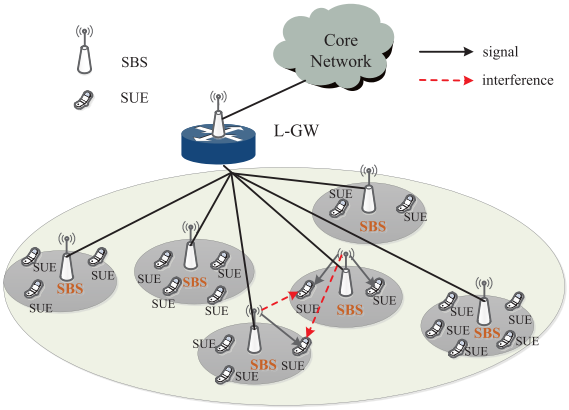

FIGURE 1. System model of the downlink DSCN Scenario.

The rest of this paper is organized as follows. Section II describes the network layout, derives the EE preference function and formulates the joint EE and ES optimization problem. The heterogeneity-aware optimization algorithm is proposed and described in detail in section III. In section IV, the performance of the proposed algorithm is evaluated and numerical results are demonstrated to verify its effectiveness. Finally, Section V concludes the paper.

II. SYSTEM MODEL AND PROBLEM FORMULATION

A. SYSTEM MODEL

In this section, we consider a DSCN consisting of S co-channel deployed SBSs, as shown in Fig. 1. A local gateway (L-GW) provides a tunnel between small cells and the internet backhaul [33].

In the DSCN, the SBS set is denoted by $\mathcal{S} = \{1, 2, \ldots, S\}$. The system has K subchannels, each one with bandwidth B_0 [Hz]. Maximum reference signal received power (RSRP) criterion is adopted for user association. The small cell user (SUE) set in the DSCN is denoted by $\mathcal{M}$ and $\mathcal{M}_s$ represents the SUE set in small cell s. We suppose that SUE m is allocated K_m subchannels and the corresponding set is $\mathcal{K}_m$. In time domain, each frame includes N subframes and the subframe set in a frame is denoted by $\mathcal{N}$. The status of subframes is indicated by a subframe configuration matrix $\mathbf{A} = [a_{sn}]_{S\times N}$, where $a_{sn} = 1$ indicates the subframe n of SBS s is active and $a_{sn} = 0$ otherwise. Similar to reference [34], perfect channel state information (CSI) is assumed.

In SBS s, assuming that SUE $m \in \mathcal{M}_s$ occupies subchannel $k \in \mathcal{K}_m$, its SINR in subframe n can be expressed as

$$\gamma_{skm}[n] = \frac{a_{sn}p_{sk}[n]\, g_{skm}}{\sum\limits_{j=1, j\neq s}^{S} a_{jn}p_{jk}[n]\, g_{jkm} + \sigma^2}, \tag{1}$$

where $p_{sk}[n]$ denotes the transmission power of SBS s on subchannel k in subframe n. The channel gain g_{skm} between SBS s and SUE m on subchannel k includes pathloss and shadowing. Since the time scale of user association is much larger than the time scale of fast fading, we do not consider

the fast fading. $I_{mk}[n] = \sum_{j=1, j\neq s}^{S} a_{jn} p_{jk}[n] g_{jkm}$ represents the co-tier interference, and σ^2 is the power of additive white Gaussian noise. Then, the transmission data rate of SUE m on subchannel k in subframe n can be calculated as

$$R_{skm}[n] = T_{sf} B_0 \log_2(1+\gamma_{skm}[n]), \tag{2}$$

where T_{sf} is the duration of each subframe. Therefore, the average data rate of SUE m in a frame is

$$R_m = \frac{1}{N} \sum_{n=1}^{N} \sum_{k \in \mathcal{K}_m} R_{skm}[n]. \tag{3}$$

To evaluate the power consumption in the DSCN, we adopt the power model in [35], which is given by:

$$P_{sk}^{total}[n] = \begin{cases} \Delta_P p_{sk}[n] + P_c, & if\ 0 < p_{sk}[n] \leq P_{sk}^{\max}[n] \\ P_s, & \text{sleep mode}, \end{cases} \tag{4}$$

where Δ_P is the inversion of power amplifier efficiency, P_c is the static dissipated power of SBS s on each subchannel, P_s is the power consumption of SBS s in sleep mode, and $P_{sk}^{\max}[n]$ is the maximum available power of SBS s on subchannel k in subframe n.

Therefore, according to the EE definition in [36], the EE of SBS s on subchannel k in subframe n can be calculated by the following formulation:

$$\eta_{sk}^{EE}[n] = \frac{R_{skm}[n]}{P_{sk}^{total}[n]} = \frac{T_{sf} B_0 \log_2(1+\gamma_{mk}[n])}{a_{sn}(\Delta_P p_{sk}[n] + P_c) + (1-a_{sn}) P_s}. \tag{5}$$

B. ENERGY EFFICIENCY PREFERENCE FUNCTION

In the DSCN, SBSs may have different EE preferences due to the heterogeneous information, such as traffic loads and number of neighbors. A SBS's traffic load is proportional to the maximum number of SUEs it serves [37]. The maximum traffic load threshold Γ is handled by SBSs and the neighbor distance threshold D_{th} is recorded by L-GW. When the Euclidean geometrical distance between two SBSs is less than D_{th}, they are considered to be neighbors. Each SBS reports its traffic loads and number of neighbors to L-GW, then the L-GW calculates their traffic load factors (TLFs) and neighbor densities (NDs), which are defined in [31].

When the traffic load of a SBS is low, then the users served by this SBS are easily satisfied and it will pay more attention to its EE optimization, resulting in high EE preference. When a SBS has many neighbors, it has more cooperation opportunities with its neighbors to sleep and reduce co-tier interference, leading to high EE preference. In order to quantify the effects of TLF ρ and ND ζ on EE, we define EE preference function as $\omega(\rho, \zeta)$. Since ρ and ζ are independent of each other, we define their impacts on EE optimization as $\omega_1(\rho)$ and $\omega_2(\zeta)$, respectively, which should have the following properties:

1) With the increase of TLF, the EE preference decreases. Therefore, $\omega_1(\rho)$ decreases with the increase on ρ, i.e., $\omega_1'(\rho) < 0$. Herein, $\omega_i'(\cdot) < 0$ is the first-order derivative of $\omega_i(\cdot) < 0$.

2) With the increase of ND, the EE preference increases. Hence, $\omega_2(\zeta)$ increases with the growth of ζ, i.e., $\omega_2'(\zeta) > 0$.

3) The EE preference becomes less sensitive to high TLF, which is that $\omega_1'(\rho)$ decreases with the increase on ρ. Therefore, $\omega_1''(\rho) < 0$. Herein, $\omega_i''(\cdot) < 0$ is the second-order derivative of $\omega_i(\cdot) < 0$.

4) The more SBS neighbors are, the more sensitive the EE preference is. Thus, $\omega_2'(\zeta)$ increase with the growth of ζ, i.e., $\omega_2''(\zeta) > 0$.

5) $\omega_1(\rho)$ and $\omega_2(\zeta)$ have the value between 0 and 1, i.e., $\omega_1(0) = 1$, $\omega_2(0) = 0$, $\omega_1(1) = 0$, and $\omega_2(1) = 1$.

Based on the above properties, similar to [38], $\omega_1(\rho)$ and $\omega_2(\zeta)$ can be defined as follows:

$$\omega_1(\rho) = \frac{e^{-b\rho} - e^{-b}}{1 - e^{-b}}, \tag{6}$$

$$\omega_2(\zeta) = \frac{e^{d\zeta} - 1}{e^{d} - 1}, \tag{7}$$

where b and d are constants which are used to adjust the slope of the curve. Accordingly, through introducing a weight factor α ($0 \leq \alpha \leq 1$), the EE preference function, $\omega(\rho, \zeta)$, can be expressed as

$$\omega(\rho, \zeta) = \alpha \omega_1(\rho) + (1 - \alpha) \omega_2(\zeta) \tag{8}$$

C. PROBLEM FORMULATION

In this paper, we aim to improve the sum of EEs with limited energy while considering the heterogeneity of SBSs through subchannel allocation, subframe configuration and power allocation. Since subchannel allocation and subframe configuration have more significant impacts on energy consumption than power allocation, and they all affect the network EE heavily, based on the EE preference function $\omega(\rho, \zeta)$ defined in Section II. B, the optimization problem can be formulated as:

$$\min_{\mathbf{A},\mathbf{K}} \sum_{n=1}^{N} \sum_{s=1}^{S} \sum_{m \in \mathcal{M}_s} \sum_{k \in \mathcal{K}_m} a_{sn}(\Delta_P p_{sk}[n] + P_c) + (1 - a_{sn}) P_s,$$

$$\max_{\mathbf{A},\mathbf{K},\mathbf{P}} \sum_{n=1}^{N} \sum_{s=1}^{S} \sum_{m \in \mathcal{M}_s} \sum_{k \in \mathcal{K}_m} \frac{\omega_s(\rho, \zeta) T_{sf} B_0 \log_2(1+\gamma_{mk}[n])}{a_{sn}(\Delta_P p_{sk}[n] + P_c) + (1 - a_{sn}) P_s},$$

$$\text{s.t.} \quad C1: R_m \geq R_m^{\min}, \quad \forall m \in \mathcal{M},$$

$$C2: \sum_{m=1}^{|\mathcal{M}_s|} K_m = K, \quad \forall s \in S,$$

$$C3: 0 \leq p_{sk}[n] \leq P_{sk}^{\max}[n], \quad \forall s \in \mathcal{S}, k \in \mathcal{K},$$

$$C4: \sum_{k=1}^{K} p_{sk}[n] \leq P_s^{\max}, \quad \forall s \in \mathcal{S},$$

$$C5: a_{sn} \in \{0, 1\}, \quad \forall s \in \mathcal{S}, n \in \mathcal{N}, \tag{9}$$

where $\mathbf{P} = [\mathbf{P}_1, \mathbf{P}_2, \ldots, \mathbf{P}_S]$ and $\mathbf{K} = [K_1, K_2, \ldots, K_M]$, C1 indicates that all SUEs' QoS should be guaranteed and

$R_m^{\min}$ is the rate requirements of SUE m, C2 is the constraint of subchannel allocation in each small cell and $|\mathcal{M}_s|$ is the cardinality of set $\mathcal{M}_s$, i.e., the number of SUEs served by SBS s, C3 is the constraint of power on each subchannel, C4 is the total power constraint of SBS and $P_s^{\max}$ is the maximum power of SBS s, C5 represents that the subframe status is a binary variable. Problem (9) is a multi-objective optimization problem. Since $\mathbf{P}$ is continuous, $\mathbf{K}$ is integer variable, and $\mathbf{A}$ is binary variable, the second objective function in problem (9) is mixed integer non-convex programming problem. Also, the coupling of $\mathbf{A}$, $\mathbf{K}$, and $\mathbf{P}$ makes problem (9) even more complicated and obtaining its global optimal solution directly is very difficult.

III. HETEROGENEITY-AWARE ENERGY SAVING AND ENERGY EFFICIENCY OPTIMIZATION

Since the computational complexity of problem (9) is NP-Hard, in this section, we propose a suboptimal heterogeneity-aware ES and EE (HESEE) algorithm by dividing it into two subproblems to get a tractable solution. First, a joint subchannel allocation and subframe configuration scheme is proposed to solve the energy minimization problem. Then, CCCP method is applied to maximize the network EE.

A. JOINT SUBCHANNEL ALLOCATION AND SUBFRAME CONFIGURATION FOR ENERGY SAVING

In the DSCN, SBSs cooperate to sleep can reduce the network energy consumption. However, the number of active subframes required to serve users and subframe configuration should be optimized. In order to consume little energy while guaranteeing different SUEs' QoS, we propose a joint subchannel allocation and subframe configuration scheme, which can be divided into the following three steps.

1) CALCULATION OF THE NUMBER OF ACTIVATED SUBFRAMES IN NON-COOPERATIVE CASE

In the non-cooperative case, we first suppose that SBSs are selfish and use maximum transmission power on all subchannels, then the energy-saving problem is formulated as follows:

$$\min_{\mathbf{A},\mathbf{K}} \sum_{n=1}^{N}\sum_{s=1}^{S}\sum_{m\in\mathcal{M}_s}\sum_{k\in\mathcal{K}_m} a_{sn}\left(\Delta_P p_{sk}[n]+P_c\right)+\left(1-a_{sn}\right)P_s,$$
$$\text{s.t.} \quad C1, C2, C5. \tag{10}$$

In order to calculate the number of active subframes for each SBS, problem (10) can be transformed into the following problem:

$$\min_{\mathbf{N}_{\text{act}},\mathbf{K}} \sum_{s=1}^{S}\sum_{m\in\mathcal{M}_s} \sum_{k\in\mathcal{K}_m} T_{sf}\left[N_{s,\text{act}}\left(\Delta_P\sum_{k=1}^{K}p_{sk}+P_c\right)+\left(N-N_{s,\text{act}}\right)P\right],$$
$$\text{s.t.} \quad C1, C2,$$
$$C5': N_{s,act}=\sum_{n=1}^{N} a_{sn}, N_{s,act}\in\{0,1,\ldots,N\}, \quad \forall s\in\mathcal{S} \tag{11}$$

where $\mathbf{N}_{\text{act}} = \left\{N_{1,\text{act}}, N_{2,\text{act}}, \ldots, N_{S,\text{act}}\right\}$ and $N_{s,\text{act}}$ is the number of active subframes in a frame for SBS s.

In the DSCN, a SUE's data rate depends on the number of active subframes of its serving SBS, i.e., $N_{sm,\text{act}}$, and the number of subchannels assigned to it, i.e., K_m. Due to the coupling between these two variables, we first calculate $N_{sm,\text{act}}$ for given K_m.

Suppose that SUE m needs $N_{sm,\text{act}}$ active subframes for data transmission, then the achievable data rate per active subframe should be $NR_m^{\min}/N_{sm,\text{act}}$. Since SUE m is allocated K_m subchannels, according to (1) and (2), the transmission power of SBS s on subchannel k in active subframe n can be expressed as

$$p_{sk}[n]=\frac{\left(I_{mk}[n]+\sigma^2\right)}{g_{skm}}\left(2^{\frac{NR_m^{\min}}{K_m B_0 T_{sf} N_{sm,\text{act}}}}-1\right), \quad \forall k\in\mathcal{K}_m. \tag{12}$$

Since the transmission power of each SBS on all subchannels is assumed to be equal, the total transmission power of SBS s to serve SUE m can be calculated as $K_m p_{sk}[n]$. For notational brevity, we define $\varphi\left(N_{sm,\text{act}}\right) \triangleq NR_m^{\min}/K_m B_0 T_{sf} N_{sm,\text{act}}$. Substituting (12) into (11) and relaxing $N_{sm,\text{act}}$ to be $0 \le N_{sm,\text{act}} \le N$, problem (11) can be reorganized as:

$$\min_{\mathbf{N}_{\text{act}}} U\left(\mathbf{N}_{\text{act}}\right)=\sum_{s=1}^{S}\sum_{m\in\mathcal{M}_s}\frac{T_{sf}\Delta_P K_m\left(I_{mk}+\sigma^2\right)}{g_{skm}/N_{sm,act}}\left(2^{\varphi\left(N_{sm,\text{act}}\right)}-1\right) + \sum_{s=1}^{S} T_{sf}\left[N_{sm,\text{act}}\left(P_c-P_s\right)+NP_s\right],$$
$$\text{s.t.} \quad C5'': N_{sm,\text{act}}\in[0,N], \quad \forall s\in S, m\in\mathcal{M}. \tag{13}$$

The second-order derivative of (13) with respect to $N_{sm,\text{act}}$ be calculated as follows:

$$\frac{\partial^2 U\left(\mathbf{N}_{\text{act}}\right)}{\partial N_{sm,\text{act}}^2}=\frac{T_{sf}\Delta_P K_m\left[\left(\ln 2\right)\varphi\left(N_{sm,\text{act}}\right)\right]^2}{g_{skm}N_{sm,\text{act}}/\left(I_{mk}+\sigma^2\right)}2^{\varphi\left(N_{sm,act}\right)}\ge 0. \tag{14}$$

Therefore, problem (13) is convex with respect to $N_{sm,act}$ and we can solve $\partial U\left(\mathbf{N}_{\text{act}}\right)/\partial N_{sm,\text{act}}=0$ to obtain the the optimal number of active subframes, which is given by

$$N_{sm,act}^{opt}=\frac{\left(\ln 2\right)NR_{m,\min}}{K_m B_0 T_{\text{sf}}\left[1+lambertw\left(\frac{g_{skm}\left(P_c-P_s\right)}{e\left(I_{mk}+\sigma^2\right)K_m\Delta_p}-\frac{1}{e}\right)\right]}. \tag{15}$$

where $lambertw(\cdot)$ is the lambert W-function, which is defined as the inverse function of $f(W)=We^W$. The detailed derivation of (15) can be found in [39].

Due to various channel conditions and the number of subchannels, different SUEs in the same SBS may need different

number of active subframes to meet their data rate requirements. Each SBS should use the maximum active subframes to guarantee all users' target data rates. Thus, the optimal number of active subframes for SBS s is

$$N_{s,\mathrm{act}}^{\mathrm{opt}} = \min\left\{\max\left\{ N_{s1,\mathrm{act}}^{\mathrm{opt}}, N_{s2,\mathrm{act}}^{\mathrm{opt}}, \ldots, N_{s|\mathcal{M}_S|,\mathrm{act}}^{\mathrm{opt}}\right\}, N\right\} \quad (16)$$

Due to the fact that $N_{s,\mathrm{act}}^{\mathrm{opt}}$ should be an integer, $N_{s,act}^{opt}$ is recalculated by $ceil(N_{s,\mathrm{act}}^{\mathrm{opt}})$.

2) FAIRNESS-BASED SUBCHANNEL ALLOCATION

Formula (15) indicates that the number of active subframes for SUE m is affected by the number of subchannels it is allocated. In each SBS, due to SUEs' random distribution and different target data rates, the number of active subframes required varies greatly. Since each SBS chooses the maximum active subframes to serve its SUEs, the subchannel allocation should be optimized to reduce the maximum active subframes its SUEs required. Therefore, the number of active subframes for SUEs within the same SBS should be fair. In this subsection, we propose a fairness-based subchannel allocation scheme.

We rewrite (15) as the following equation for simplicity:

$$N_{sm,act}^{opt} = \frac{X_m}{K_m\left[1+lambertw\left(Y_m/K_m - Z\right)\right]}, \quad (17)$$

where $X_m = (\ln 2)\, NR_{m,\min}/K_m B_0 T_{\mathrm{sf}}$, $Z = 1/e$, and $Y_m = g_{skm}\left(P_c - P_s\right)/e\left(I_{mk}+\sigma^2\right)\Delta_p$. In order to make SUEs in the same SBS have fair active subframes, $N_{s1,act}^{opt} = N_{s2,act}^{opt} = \cdots = N_{s|\mathcal{M}_s|,act}^{opt}$ should be satisfied. However, since (17) is complex, it is difficult to obtain the optimal subchannel allocation scheme $\mathbf{K}^*$.

Notice that the influence of K_m on $lambertw(\cdot)$ is usually smaller than Y_m, we introduce a simple approximate proportional form that is easy to handle, which is given by

$$\tilde{N}_{sm,act}^{opt} = \frac{X_m}{K_m\left[lambertw\left(Y_m - Z\right)\right]}. \quad (18)$$

To guarantee fair active subframes among SUEs in the same SBS, i.e., $\tilde{N}_{s1,act}^{opt} = \tilde{N}_{s2,act}^{opt} = \cdots = \tilde{N}_{s|\mathcal{M}_s|,act}^{opt}$, we have

$$\begin{aligned}\frac{X_1/K_1}{lambertw\left(\bar{Y}_1\right)} &= \frac{X_2/K_2}{lambertw\left(\bar{Y}_2\right)} \\ &= \cdots = \frac{X_{|\mathcal{M}_s|}/K_{|\mathcal{M}_s|}}{lambertw\left(\bar{Y}_{|\mathcal{M}_s|}\right)}, \end{aligned} \quad (19)$$

where $\bar{Y}_m = Y_m - Z$. Accordingly, the fairness-based subchannel allocation scheme can be obtained as follows:

$$K_m = \frac{X_m/lambertw\left(\bar{Y}_m\right)}{\sum_{m=1}^{|\mathcal{M}_s|}\left[X_m/lambertw\left(\bar{Y}_m\right)\right]}, \forall m \in \mathcal{M}_s, s \in S. \quad (20)$$

Equation (20) suggests that SUEs with larger target data rates and worse channel conditions would be assigned more subchannels. Therefore, the SUEs within the same SBSs can have fair number of active subframes and their data requirements can be guaranteed. The fairness-based subchannel allocation scheme is given by Algorithm 1.

In Algorithm 1, in order to obtain the number the active subframes for each SBS, the transmission power on each subchannel in each SBS is assumed to be the maximum value, i.e., $P_{sk}^{\max}, \forall s \in \mathcal{S}, k \in \mathcal{K}$. As shown in step 2-5, in the DSCN, users choose their serving SBSs based on the maximum RSRP criterion. Therefore, we can obtain the SUE set served by each SBS. In order to make each SBS activate as few subframes as possible while ensuring all users' target data rates, the subchannel allocation for SUEs within the same SBS should be optimized. Step 6-12 demonstrate the subchannel allocation process. In each SBS, SUEs calculate the co-tier interference they suffered. Then the interference and data rate requirements are reported to each SBS by its serving SUEs. Thus, each SBS can calculate the values of X_m and $\bar{Y}_m$. According to equation (20), the number of subchannels required by each SUEs can be calculated. Then, each SBS can allocate a corresponding number of continuous subchannels to its service SUEs. For the sake of convenience, we use $u(s,k)$ to denote the SUE occupied subchannel k in SBS s.

3) GROUP-BASED SUBFRAME CONFIGURATION

Substituting (20) into (17), the optimal number of active subframes can be calculated as

$$N_{sm,act}^{opt} = \frac{lambertw\left(\bar{Y}_m\right)\sum_{m=1}^{|\mathcal{M}_s|}\left[X_m/lambertw\left(\bar{Y}_m\right)\right]}{1+lambertw\left[\frac{\sum_{m=1}^{|\mathcal{M}_s|}\left[X_m/lambertw(\bar{Y}_m)\right]}{X_m/\left[Y_m lambertw(\bar{Y}_m)\right]} - Z\right]}. \quad (21)$$

For each SBS, the optimal number of active subframes can be calculated by (21) and (16). Since the positions of active subframes can affect the co-tier interference, the subframe configuration should be optimized. In order to alleviate the co-tier interference between SBSs, SBSs can cooperate to form groups and conduct reasonable subframe configuration. Therefore, in this subsection, a group-based subframe configuration algorithm is presented.

When a SBS has large EE preference weight, it should form groups with its neighbors first in order to obtain more sleep opportunities. Therefore, the EE preference should be considered in the group formation process. Before forming groups, the L-GW characterizes all SBSs' heterogeneous information, i.e., ρ and ζ, and calculates their EE preference weights $\omega(\rho,\zeta)$ based on (6)-(8).

Algorithm 2 describes the proposed group-based subframe configuration algorithm. The initial group structures are initialized, which includes S groups with only one SBS in each group. Based on the EE preference weights, the initial groups are arranged in a weight list in descending order. Then, each SBS identifies the strongest interfering SBS from its neighbor SBSs. Step 4-14 show the process of group formation. Each group in the weight list tries to form new groups with its strongest interfering SBS by sending group formation

Algorithm 1 Fairness-Based Subchannel Allocation Algorithm

Input: SUEs' target data rate $R_m^{\min}, \forall m \in \mathcal{M}$.
Output: the optimal subchannel allocation $\mathbf{K}^*$.

1: Initialize the initial transmission power of each subchannel as $P_{sk}^{\max}, \forall s \in \mathcal{S}, k \in \mathcal{K}$.
2: **for** $m = 1 : M$ **do**
3: User m measures the RSRP value from all SBSs and choose its serving SBS according to the maximum RSRP criterion.
4: The SUE set served by SBS s is denoted by $\mathcal{M}_s$.
5: **end for**
6: **for** $s = 1 : S$ **do**
7: **for** $m = 1 : |\mathcal{M}_s|$ **do**
8: SUE m reports its target data rate and the interference it suffered to SBS s.
9: **end for**
10: SBS s calculates X_m and parameter $\bar{Y}_m, m \in \mathcal{M}_s$.
11: According to (20), SBS s calculates the number of subchannels required by SUE m, i.e., K_m, and assigns K_m continuous subchannels to SUE m. In SBS s, if a SUE is assigned to subchannel k, we denote it as $u(s,k)$.
12: **end for**

request. If the strongest interfering SBS receives the request and does not form groups with others, it will accept the request and form a new group with the SBS. Accordingly, the group structure is updated. Noth that an interfering SBS may receive several requests from more than one SBSs, it only chooses the SBS with the highest EE preference weight to cooperate by responding group formation acknowledge message to the SBS. Meanwhile, it responses group formation failure message to other SBSs sending requests. Otherwise, if the interfering SBS has formed groups with others, it will refuse the request and responses group formation failure message. Step 15-25 demonstrate the subframe configuration. Suppose that SBSs in the DSCN form the final group structure $\tilde{\mathcal{G}} = \left\{\tilde{\mathcal{G}}_1, \tilde{\mathcal{G}}_2 \ldots, \tilde{\mathcal{G}_{G_C}}\right\}$, where G_C denotes the total number of groups. Note that the groups in $\tilde{\mathcal{G}}$ are not overlapped, i.e., $\tilde{\mathcal{G}}_i \neq \emptyset, \tilde{\mathcal{G}}_j \neq \emptyset, \tilde{\mathcal{G}}_i \cap \tilde{\mathcal{G}}_j = \emptyset, \forall i \neq j$. If there are two SBSs in the same group, they will be assigned orthogonal active subframes. Since the implementation of frame-level synchronization is beyond the scope of this paper, the strict synchronization among SBSs is assumed to be guaranteed.

Compared with non-cooperative scheme, SBSs can use orthogonal active subframes with its strongest interfering SBS to serve users. Therefore, the co-tier interference can be mitigated and less transmission power is required to meet users' target data rates.

B. POWER ALLOCATION FOR HETEROGENEITY-AWARE SYSTEM EE OPTIMIZATION

When the optimal subchannel allocation $\mathbf{K}^*$ and subframe configuration $\mathbf{A}^*$ are obtained, we focus on the system EE maximization problem in (9), which is equivalent to maximize the system EE in each subframe. Specifically, in subframe n, the optimization problem is:

$$\begin{aligned}
&\max_{\mathbf{P}[n]} \sum_{s=1}^{S}\sum_{k=1}^{K} \omega_s(\rho,\zeta)\,\eta_{sk}^{EE}[n],\\
&s.t.\ C1': R_{skm}[n] \geq \frac{a_{sn} N R_m^{\min}}{N_{sm,\mathrm{act}} K_m}, \quad \forall m \in \mathcal{M}, k \in \mathcal{K}_m,\\
&\quad C3: 0 \leq p_{sk}[n] \leq P_{sk}^{\max}, \quad \forall s \in \mathcal{S}, k \in \mathcal{K},\\
&\quad C4: \sum_{k=1}^{K} p_{sk}[n] \leq P_s^{\max}, \quad \forall s \in \mathcal{S}.
\end{aligned} \tag{22}$$

Notice that problem (22) is non-convex due to the sum-of-ratios in the objective function, which makes it arduous to be addressed directly.

Similarly, according to [40], we introduce a new matrix $\boldsymbol{\psi}[n] = \{\psi_{sk}[n]\}_{S\times K}$. Then problem (22) can be converted into the following problem:

$$\begin{aligned}
&\max_{\mathbf{P}[n]} \sum_{s=1}^{S}\sum_{k=1}^{K} \psi_{sk}[n],\\
&s.t.\ C1', C3, C4,\\
&\quad C6: \frac{\omega_s(\rho,\zeta) R_{skm}[n]}{P_{sk}^{total}[n]} \geq \psi_{sk}[n].
\end{aligned} \tag{23}$$

To solve problem (23), we introduce Theorem 1 [40] and use ω_s to replace $\omega_s(\rho,\zeta)$ in the following.

Theorem 1: If $\left(\mathbf{P}^*[n], \boldsymbol{\psi}^*[n]\right)$ is the optimal solution to (23), then there exist $\chi_{sk}^*[n], s = 1, \ldots, S, k = 1, \ldots, K$, such that $\mathbf{P}^*[n]$ is a solution to the following problem:

$$\begin{aligned}
&\max_{\mathbf{P}[n]} \sum_{s=1}^{S}\sum_{k=1}^{K} \chi_{sk}[n]\left\{\omega_s R_{skm}[n] - \psi_{sk}[n] P_{sk}^{total}[n]\right\},\\
&s.t.\ C1', C3, C4, C6.
\end{aligned} \tag{24}$$

Furthermore, $\mathbf{P}^*[n]$ satisfies the following equations for $\boldsymbol{\chi}[n] = \boldsymbol{\chi}^*[n]$ and $\boldsymbol{\psi}[n] = \boldsymbol{\psi}^*[n]$,:

$$\chi_{sk}[n] = \frac{1}{P_{sk}^{total}[n]}, \psi_{sk}[n] = \frac{\omega_s R_{skm}[n]}{P_{sk}^{total}[n]}, \quad \forall s \in \mathcal{S}, k \in \mathcal{K}. \tag{25}$$

Proof: See Appendix A.

Theorem 1 implies that the optimal solution of (23) can be obtained by solving problem (24). Furthermore, we can rewrite the non-convex constraint $C1'$ into its equivalent convex linear form as

$$C1'': p_{sk}[n] g_{skm} + \left(1 - 2^{\frac{N R_m^{\min}}{N_{sm,\mathrm{act}} K_m B_0}}\right)\left(I_{mk}[n] + \sigma^2\right) \geq 0. \tag{26}$$

Now, we rearrange the objective function in (24) as $U(\mathbf{P}[n]) = U_{cave1}(\mathbf{P}[n]) - U_{cave2}(\mathbf{P}[n])$, then, problem (24) is equivalent to the following problem:

$$\max_{\mathbf{P}[n]} U(\mathbf{P}[n]),$$

Algorithm 2 Group-Based Subframe Configuration Algorithm

Input: SUEs' target data rate $R_m^{\min}, \forall m \in \mathcal{M}$, subchannel allocation $\mathbf{K}^*$, SBSs' EE preference weights $\omega(\rho, \zeta)$.

Output: the final group structure $\tilde{\mathcal{G}}$ and the optimal subframe configuration $\mathbf{A}^*$.

1: Initialize the initial group structure $\mathcal{G} = \{\mathcal{G}_1, \mathcal{G}_2 \ldots, \mathcal{G}_s, \ldots, \mathcal{G}_S\}$, where the member of $\mathcal{G}_s$ is SBS s. Initialize the final group structure $\tilde{\mathcal{G}} = \mathcal{G}$.
2: All groups are stored in the weight list $\mathcal{G}^{\text{wei}} = \left\{\mathcal{G}_1^{\text{wei}}, \mathcal{G}_2^{\text{wei}}, \ldots, \mathcal{G}_S^{\text{wei}}\right\}$, where their EE preference weights $\omega(\rho, \zeta)$ are from large to small.
3: Each SBS s, $s \in \mathcal{S}$, identifies its strongest interfering SBSs $\mathcal{L}_{s,\text{inf}}$ by resorting to a SUE.
4: **for** $ele = 1 : |\mathcal{G}_S|$ **do**
5: Obtain SBS $s = \mathcal{G}_{ele}^{\text{wei}}$, i.e., the element in the $\mathcal{G}_{ele}^{\text{wei}}$.
6: **if** SBS s has not formed groups with others **then**
7: SBS s sends group formation request to its strongest interfering SBS $\mathcal{L}_{s,\text{inf}}$.
8: **if** SBS $\mathcal{L}_{s,\text{inf}}$ receives group formation request and has not formed groups with others **then**
9: The new group $\tilde{\mathcal{G}}$ is formed,i.e., $\tilde{\mathcal{G}} = s \cup \mathcal{L}_{s,\text{inf}}$ and SBS $\mathcal{L}_{s,\text{inf}}$ responses group formation acknowledge message to the cooperative SBS.
10: **else**
11: The new group can not be formed and SBS $\mathcal{L}_{s,\text{inf}}$ responses group formation failure message to the SBSs sending requests.
12: **end if**
13: **end if**
14: **end for**
15: **for** $g = 1 : \left|\tilde{\mathcal{G}}\right|$ **do**
16: **if** There is only one SBS in $\tilde{\mathcal{G}}_g$ **then**
17: Assign random active subframes for this SBS.
18: **else**
19: **if** There are two SBSs in $\tilde{\mathcal{G}}_g$, i.e., SBS i and j, and the total number of active subframes for SBS i and j is not larger than N **then**
20: Assign orthogonal active subframes for SBS i and j.
21: **else**
22: Assign orthogonal active subframes for these SBSs proportionately, i.e., assign $\left\lfloor N_{si,act}^{opt} N \Big/ \left(N_{si,act}^{opt} + N_{sj,act}^{opt}\right) \right\rfloor$ active for SBS i, and $N - \left\lfloor N_{si,act}^{opt} N \Big/ \left(N_{si,act}^{opt} + N_{sj,act}^{opt}\right) \right\rfloor$ subframes to SBS j.
23: **end if**
24: **end if**
25: **end for**

$$s.t.\ C1'', C3, C4, C6, \tag{27}$$

where both $U_{cave1}(\mathbf{P}[n])$ and $U_{cave2}(\mathbf{P}[n])$ are concave, and $U_{cave1}(\mathbf{P}[n]) = \sum_{s=1}^{S}\sum_{k=1}^{K} \chi_{sk}[n]\,\omega_s B_0 \log_2\left(\sum_{t=1}^{S} p_{tk}[n]\, g_{tkm} + \sigma^2\right)$ and $U_{cave2}(\mathbf{P}[n]) = \sum_{s=1}^{S}\sum_{k=1}^{K} \chi_{sk}[n]\,\omega_s B_0 \log_2\left(I_{mk}[n] + \sigma^2\right) + \sum_{s=1}^{S}\sum_{k=1}^{K} \chi_{sk}[n]\,\psi_{sk}[n]\, P_{sk}^{total}[n]$. Thus, $U(\mathbf{P}[n])$ is a difference-of-convex function. Therefore, problem (27) can be addressed by CCCP method and we introduce Theorem 2 [41].

Theorem 2: The solution to problem (27) can be obtained by tackling the following sequence of convex programs:

$$\mathbf{P}^{(l+1)}[n] = \arg\max_{\mathbf{P}[n]} \left\{ U_{cave1}(\mathbf{P}[n]) - \mathbf{P}^T[n] * \nabla U_{cave2}\left(\mathbf{P}^{(l)}[n]\right) \right\}, \tag{28}$$

where $\mathbf{P}^T[n]$ denotes the transpose of $\mathbf{P}[n]$ and $\nabla U_{cave2}\left(\mathbf{P}^{(l)}[n]\right) = \left[\nabla_1^{(l)}[n], \nabla_2^{(l)}[n], \ldots, \nabla_K^{(l)}[n]\right]$ denotes the gradient of $U_{cave2}(\mathbf{P}[n])$ at $\mathbf{P}^{(l)}[n]$ where

$$\nabla_k^{(l)}[n] = \sum_{j=1, j\neq s}^{S} \frac{B_0 \chi_{jk}[n]\,\omega_j g_{sku(j,k)} \big/ \ln 2}{\sum_{t=1, t\neq j}^{S} p_{tk}[n]\, g_{tku(j,k)} + \sigma^2} + \Delta_p \chi_{sk}[n]\,\psi_{sk}[n] \triangleq L_{sk}(\chi_{sk}, \psi_{sk})[n].$$

Proof: See Appendix B.

According to Theorem 2, problem (27) has been transformed into a standard convex optimization problem (28) and we can obtain the optimal power as

$$p_{sk}^*[n] = \left[\frac{B_0 \chi_{sk}[n]\,\omega_s \big/ \ln 2}{L_{sk}(\chi_{sk}, \psi_{sk})[n] + \lambda_s - \mu_{sk}} - \frac{I_{mk}[n] + \sigma^2}{g_{skm}} \right]_0^{P_{sk}^{\max}[n]}, \tag{29}$$

where $\mu_{sk} = \nu_{sk} g_{skm} + \sum_{j=1, j\neq s}^{S} \nu_{jk} g_{sku(j,k)} \left(1 - 2^{\frac{NR_{u(j,k)}^{\min}}{N_{s,\text{act}} K_{u(j,k)} B_0}}\right)$, $\boldsymbol{\nu}$ and $\boldsymbol{\lambda}$ are Lagrange multiplier vectors. The heterogeneity-aware energy efficient power allocation algorithm is summarized in Algorithm 3. According to [41], the CCCP algorithm can start at some random point in the feasible set, $P^{(0)}[n] = \left\{p_{sk}^{(0)}[n]\right\}_{S\times K}$, where $p_{sk}^{(0)}[n]$ should subject to constraints $C1''$, $C3$, $C4$ and C6. We assume that the interfering SBSs use maximum transmission power and set $p_{sk}^{(0)}[n] = \left[\frac{NR_m^{\min}}{(2^{\frac{NR_m^{\min}}{N_{sm,\text{act}} K_m B_0}} - 1)(I_{mk}[n] + \sigma^2)} \Big/ g_{skm}, P_{sk}^{\max} \right]_0^{P_{sk}^{\max}[n]}, \forall s \in \mathcal{S}, k \in \mathcal{K}.$

C. COMPLEXITY ANALYSIS

The proposed HESEE algorithm includes three algorithms, which are fairness-based subchannel allocation in Algorithm 1, group-based subframe configuration in Algorithm 2, and heterogeneity-aware energy efficient power allocation in Algorithm 3. The complexity of subchannel allocation in Algorithm 1 is $O(S|\mathcal{M}_s|)$. In Algorithm 2, EE preference weights of S SBSs are sorted

Algorithm 3 Heterogeneity-Aware Energy Efficient Power Allocation Algorithm

Input: SUEs' target data rate $R_m^{\min}, \forall m \in \mathcal{M}$, EE preference weights $\omega_s(\rho, \zeta), \forall s \in \mathcal{S}$, subchannel allocation $\mathbf{K}^*$, subframe configuration $\mathbf{A}^*$, maximum number of iterations $L_{\max}$, and the algorithm accuracy indicator $\varepsilon > 0$.

Output: the optimal power allocation $\mathbf{P}^*$.

1: **for** $n = 1 : N$ **do**
2: Initialize $l = 0$ and $P^{(0)}$. Calculate $\chi_{sk}^{(0)}[n]$ and $\psi_{sk}^{(0)}[n], \forall s \in \mathcal{S}, k \in \mathcal{K}$ based on (25).
3: **repeat**
4: Solve problem (27) by CCCP method, obtain the optimal power $p_{sk}^*[n]$ according to (29).
5: Update $\chi_{sk}^{(l)}[n]$ and $\psi_{sk}^{(l)}[n]$.
6: Set $l = l+1$
7: **until** $\left| \max\limits_{\mathbf{P}[n]} \left\{ \sum\limits_{s=1}^{S} \chi_{sk}^{(l)}[n] \left(\omega_s R_{skm}^{(l)}[n] - \psi_{sk}^{(l)}[n] P_{sk}^{total,(l)}[n] \right) \right\} \right| < \varepsilon$ *or* $l = L_{\max}$.
8: **end for**

by L-GW and the according complexity is $O\left(S\log_2 S\right)$. Assuming that SBSs form G_C groups, then the complexity of group-based subframe configuration scheme is $O\left(G_C NS\log_2 S\right)$. In Algorithm 3, the complexity of CCCP method is $O\left(\log_2\left(1/\varepsilon\right)\right)$. Suppose that the required number of iterations for updating $(\boldsymbol{\chi}[n], \boldsymbol{\psi}[n])$ and subgradient method are $L_{\boldsymbol{\chi},\boldsymbol{\psi}}^{\text{iter}}$ and $L_{\text{sg}}^{\text{iter}}$, respectively, the complexity of Algorithm 3 is $O\left(SKNL_{\boldsymbol{\chi},\boldsymbol{\psi}}^{\text{iter}} L_{\text{sg}}^{\text{iter}} \log_2\left(1/\varepsilon\right)\right)$. Therefore, the total complexity of HESEE algorithm in the worst condition is $O\left(S|\mathcal{M}_s| + G_C NS\log_2 S + SKNL_{\boldsymbol{\chi},\boldsymbol{\psi}}^{\text{iter}} L_{\text{sg}}^{\text{iter}} \log_2\left(1/\varepsilon\right)\right)$. Since N, K, $|\mathcal{M}_s|$, G_C, $L_{\boldsymbol{\chi},\boldsymbol{\psi}}^{\text{iter}}$ and $L_{\text{sg}}^{\text{iter}}$ are usually small values, the HESEE algorithm can be well implemented in practice.

IV. NUMERICAL RESULTS

A. SIMULATION SETTINGS

In this section, the system level numerical simulation is developed via Monte-Carlo methods to illustrate the performance of the HESEE scheme. In the simulation setup, S SBSs are randomly deployed in a $100*100m^2$ area. SUEs' target data rates are chosen from the set $\{ R_i | R_i = (0.5i)\,Mbps, i = 1 : 10 \}$. The OFDM-based downlink transmission is investigated. The simulation parameters referenced from [42]. In particular, main simulation parameters are listed in Table 1. Unless otherwise specified, we set $\alpha = 0.5$ in the following simulations.

B. FAIRESS EVALUATION

In order to evaluate the fairness among SUEs in subframe configuration for HESEE scheme, we introduce Jain's index [43], which is given by:

$$f\left(N_{sm,act}^{opt}\right) = \frac{\left(\sum\limits_{m=1}^{|\mathcal{M}_s|} N_{sm,act}^{opt}\right)^2}{|\mathcal{M}_s| \sum\limits_{m=1}^{|\mathcal{M}_s|} \left(N_{sm,act}^{opt}\right)^2}, \quad \forall s \in \mathcal{S}. \tag{30}$$

The fairness index value ranges from 0 to 1, and the larger value means the more fair case.

TABLE 1. Simulation parameters.

Parameter	Value
Carrier frequency	3.5 GHz
Maximum transmission power of SBS	30dBm
System bandwidth B	10 MHz
Number of users	100
Number of subchannels K	50
Number of subframes per frame N	10
Subframe duration T_{sf}	1ms
Noise power spectral density	−174dBm/Hz
Small cell path loss model	$140.7 + 36.7\log 10(d[\text{km}])$dB
Log-normal shadowing fading	10 dB
Traffic model	Full Buffer
Power consumption $\Delta_P/P_c/P_s$ [35]	4.0/0.136W/4.3W
b/d	3.0/3.0
Maximum traffic load threshold Γ	15
Maximum distance threshold D_{th}	30m
Maximum number of iterations $L_{\max}$	100

C. SIMULATION RESULTS

In the following, we compare HESEE scheme with other schemes, which are:

1) Round robin based subchannel allocation (RRSA) scheme: All SUEs within a SBS are assigned subchannels in round robin way. Group-based subframe configuration is considered and transmission power is optimized to improve system EE.

2) Base scheme: Fairness-based subchannel allocation algorithm is adopted. All SBSs are active in all subframes and transmit with maximum power.

3) ES scheme: Fairness-based subchannel allocation and group-based subframe configuration are considered. Power allocation is optimized to minimize energy consumption.

4) EE maximum (MaxEE) scheme: Fairness-based subchannel allocation and non-cooperative subframe configuration are considered. Power allocation is optimized to maximize the system EE.

5) Equal weighted ES and EE optimization (EWESEE) scheme: Fairness-based subchannel allocation and group-based subframe configuration are considered. All SBSs have equal EE preference weights and power allocation is optimized to maximize the system EE.

In RRSA, Base, ES and MaxEE schemes, different EE preference weights are considered.

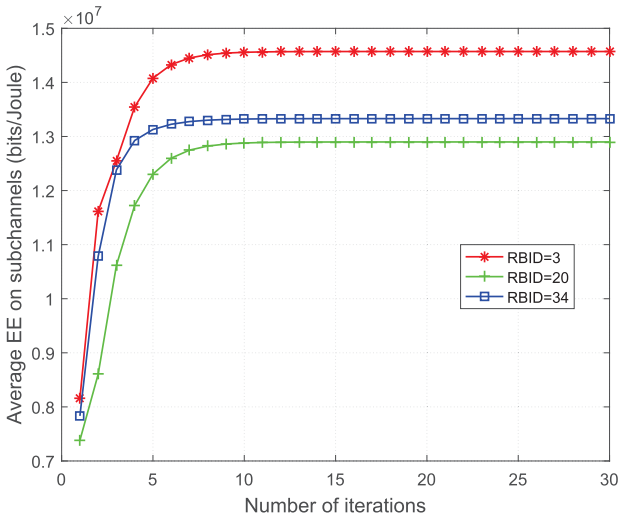

FIGURE 2. Convergence of the HESEE scheme on different subchannels.

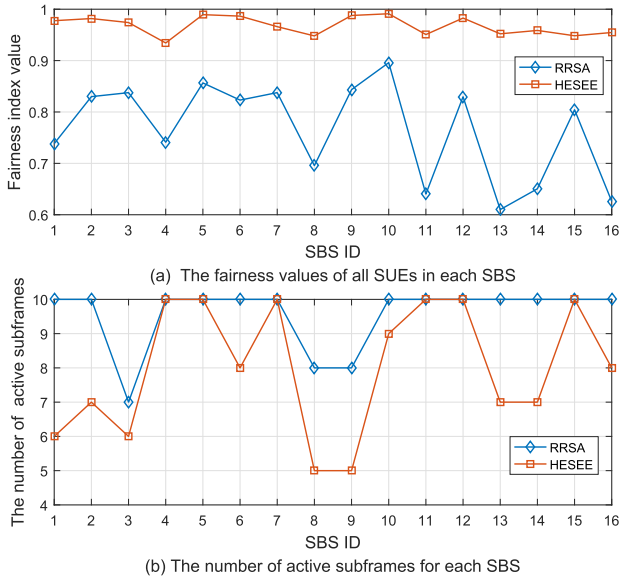

FIGURE 3. Fairness values of SUEs and the number of active subframes for SBSs.

In Fig. 2, the convergence of HESEE scheme is evaluated when the number of SBSs is 16. It can be seen from Fig. 2 that the average EEs on some random subchannels in a random subframe all converge after 12 iterations.

Fig. 3 shows the fairness values of SUEs and the number of active subframes for SBSs in the DSCN with 16 SBSs. From Fig. 3(a), we can see that the fairness in all SBSs in the HESEE scheme are above 0.93 while it is below 0.9 in the RRSA scheme. Therefore, our proposed fairness-based subchannel allocation algorithm is efficient in guaranteeing fair number of active subframes between SUEs within the same SBS. In addition, the SBSs need less active subframes to meet users' data rate requirements in the HESEE scheme, as shown in Fig. 3(b).

Fig. 4 illustrates SUE satisfaction in the HESEE scheme. The ratio of satisfied SUEs is defined as the the proportion of SUEs whose target data rates are satisfied to the total number

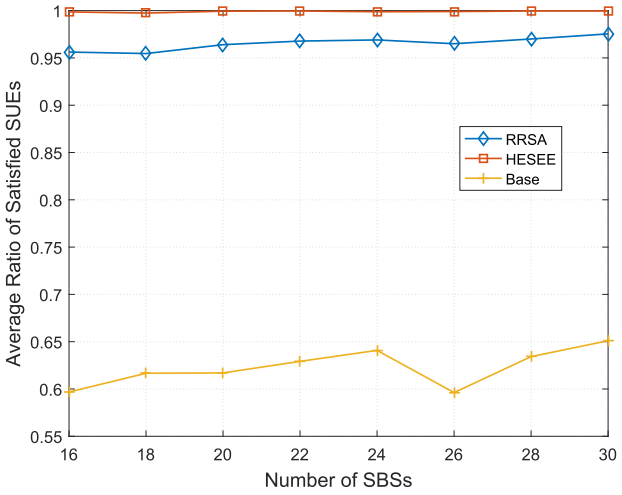

FIGURE 4. SUE satisfaction versus network density.

of SUEs. It can be seen that the ratio of satisfied SUEs in the HESEE scheme is more than 99.7% while the values are less than 97.5% and 65.1% in the RRSA and Base schemes, respectively. Therefore, our proposed HESEE scheme can guarantee more SUEs' data rate requirements via optimizing transmission power and assigning more subchannels to SUEs with larger rate requirements and worse channel conditions.

Fig. 5 shows the effects of heterogeneous information on EE in the HESEE scheme. As a comparison, the performance of EWESEE scheme is also given. Although all SBSs have equal EE preference weights in the EWESEE scheme, they obtain different EE due to various channel conditions. Table 2 presents the TLF, ND and EE preference weights of SBSs. In order to evaluate the influences of TLF and ND on EE, we set different weights in the following simulations.

1) Fig. 5 (a) presents the influence of TLF on EE through setting $\alpha = 1.0$. We can see that the EEs of SBS 3, 5, 6, and 9 in HESEE scheme are larger than that in EWESEE scheme. This is because these SBSs have lower traffic loads, resulting in larger EE preference weights than others in the HESEE scheme as shown in Table 2 while all SBSs have equal weights in the EWESEE scheme. Instead, SBS 1 and 8 obtain much lower EE in the HESEE scheme due to lower EE preference weights. Therefore, SBSs with lower traffic load can attain higher EE in the HESEE scheme and the EEs of SBSs can be adjusted based on their TLFs.

2) The impact of ND on EE is evaluated in Fig. 5 (b) where $\alpha = 0$. The EE preference weight $\omega(\rho, \zeta) = 1.00$ in Table 2 means that the SBS has the maximum neighbors. It can be observed that SBS 4, 7, and 10 obtain higher EE in the HESEE scheme compared with the EWESEE scheme. Meanwhile, SBS 1 and 5 attain less EE because of lower EE preference weights. Therefore, SBSs with more neighbors can obtain higher EE in the HESEE scheme and the EEs of SBSs can be optimized based on their NDs.

3) In order to evaluate the co-effects of TLF and ND on EE, we set $\alpha = 0.5$ in Fig. 5 (c). Since the EE preference weights of SBS 4, 6, 7, 9, and 10 are much larger than others

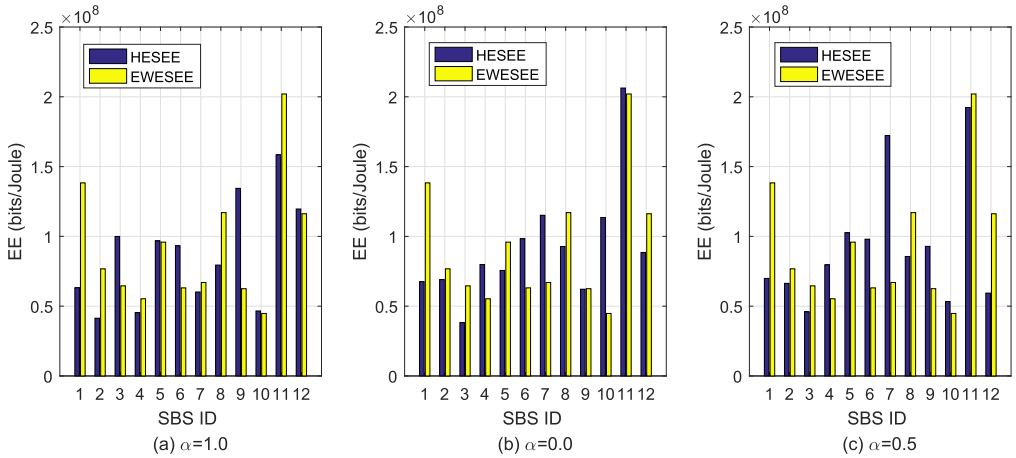

FIGURE 5. EE of SBSs for different weights of heterogeneous information in one drop.

TABLE 2. Heterogeneous information and EE preference weights of SBSs in HESEE scheme.

SBS ID	1	2	3	4	5	6	7	8	9	10	11	12
TLF (ρ)	0.90	0.67	0.33	0.67	0.33	0.13	0.67	0.87	0.33	0.60	0.53	0.53
ND (ζ)	0.25	0.50	0.50	1.00	0.25	0.75	1.00	0.75	0.75	1.00	0.75	0.50
$\omega(\rho,\zeta)$ when α=1.0	0.02	0.09	0.33	0.09	0.33	0.65	0.09	0.03	0.33	0.12	0.16	0.16
$\omega(\rho,\zeta)$ when α=0	0.06	0.18	0.18	1.00	0.05	0.44	1.00	0.44	0.44	1.00	0.44	0.18
$\omega(\rho,\zeta)$ when α=0.5	0.04	0.14	0.26	0.55	0.20	0.55	0.55	0.24	0.39	0.56	0.30	0.17

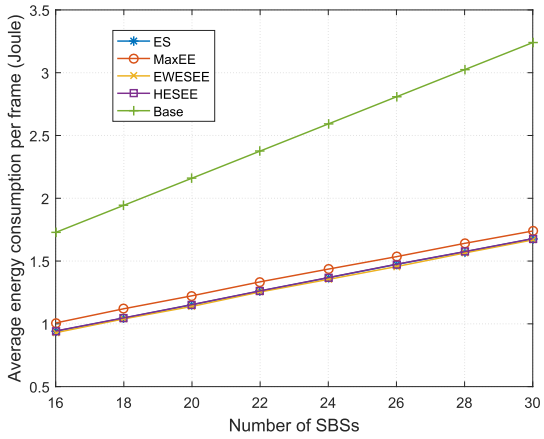

FIGURE 6. Average network energy consumption versus network density.

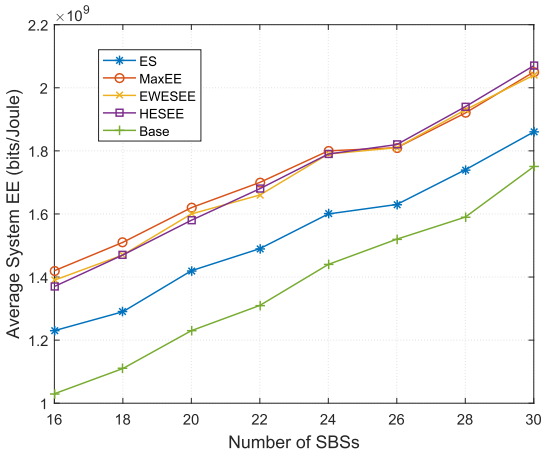

FIGURE 7. Average system EE versus network density.

in Table 2, the EEs of these SBSs can be largely improved in the HESEE scheme. Thus, our proposed HESEE scheme can optimize the SBSs' EEs based on their TLFs and NDs adaptively. In addition, the weights of TLF and ND can be adjusted as desired.

In order to evaluate the performance of group-based subframe configuration and power allocation in the HESEE scheme, the average network energy consumption and system EE with respect to network density are shown in Fig. 6 and Fig. 7, respectively.

In Fig. 6, we can find that the energy consumption increases with the increase of network density in all schemes. Since SBSs do not sleep in the Base scheme, energy consumption is the largest. Since SBSs cooperate with their neighbors to sleep in more subframes and power allocation is optimized to further reduce energy consumption in the ES scheme, its energy consumption is the smallest. Our proposed HESEE scheme consumes almost the same energy as the ES scheme. The reason is that the sleep strategies of these two schemes are the same and the transmission power is only a small part of the total energy consumption. Compared with the Base and MaxEE schemes, the HESEE scheme can reduce the network energy consumption by up to 48.2% and 6.5%, respectively. Therefore, our proposed HESEE scheme can save the network energy significantly.

As shown in Fig. 7, the system EE in all schemes increases with the growth of the network density due to the spectrum reuse. Compared with the ES scheme, the HESEE scheme can

improve the system EE by up to 13.5%. This is because the transmission power is optimized to improve the system EE in the HESEE scheme. Compared with the MaxEE scheme, the HESEE scheme decreases the system EE by 3.4% when the number of SBSs is 16. when the number of SBSs is over 24, the HESEE scheme can achieve larger EE than the MaxEE scheme. The reason is that SBSs use less active subframes to serve users by forming groups to sleep in the HESEE scheme and the co-rier interference can be efficiently mitigated in the denser network. Therefore, our proposed HESEE scheme can improve the system EE greatly through cooperating to sleep and energy-efficient power optimization in the DSCN.

From Fig. 6 and Fig. 7, we can observe that the system EE is seriously degraded in the ES scheme when SBSs cooperate to sleep and the transmission power is optimized to minimize the network consumption. However,our proposed HESEE scheme can consume almost the same energy with the ES scheme while improve the system EE by up to 13.5% through optimizing the transmission power in the active subframes to maximize the system EE. On the other hand, compared with the MaxEE scheme, our proposed HESEE scheme can improve system EE with less energy when the number of SBSs is over 24. Therefore, the transmission power of SBSs are utilized efficiently in the HESEE scheme.

V. CONCLUSION

This paper has investigated joint subchannel allocation, subframe configuration and power allocation to save energy and optimize EE simultaneously while considering SBSs' heterogeneity. Firstly, the impacts of heterogeneous information on EE are characterized as the EE preference function. Then, the joint ES and EE optimization is formulated as a multi-objective optimization problem, which is tackled by the proposed HESEE algorithm. Fairness-based subchannel allocation and group-based subframe configuration are performed to reduce the network energy consumption, and energy-efficient power allocation is optimized with the CCCP method. Simulation results illustrate that SBSs' EEs can be optimized based on their EE preferences. In addition, the HESEE scheme obtains better EE performance with less energy consumption.

In the practical system, due to the pilot contamination and high computational complexity, achieving accurate CSI is difficult, we will study the effects of imperfect CSI on energy efficient resource allocation in the future work. Caching content on SBSs can relief the pressure of backhaul and reduce the transmission latency. Mobile edge computing (MEC) can reduce the computing burden of SUEs. Therefore, caching and MEC have been widely investigated. However, the serious interference in the DSCN would degrade the performance. In [44] and [45], the authors study the interference alignment in the DSCN with caching and computing. Since the caching energy consumption and computing energy consumption in the DSCN cannot ignored, we will focus on the green communications in the DSCN with caching and computing in the future. In addition, since the numbers of SBSs and SUEs become huge, we will explore methods from the domain of machine learning to realize green communications for the next wireless communication networks.

APPENDIX A
PROOF OF THEOREM 1

The constraint C6 in problem (23) is equivalent to:

$$\omega_s R_{skm}[n] - \psi_{sk}[n] P_{sk}^{total}[n] \geq 0. \tag{31}$$

For the problem (22), we define the following function:

$$\begin{aligned} &L(\mathbf{P}[n], \alpha, \boldsymbol{\beta}, \boldsymbol{\theta}, \boldsymbol{\chi}[n]) \\ &= \sum_{s=1}^{S}\sum_{k=1}^{K} \beta_{mk}\left[p_{sk}[n] g_{skm} + \left(1 - 2^{\frac{NR_m^{\min}}{B_0 N_{sm,act} K_m}}\right)\left(I_{mk} + \sigma^2\right)\right] \\ &\quad + \alpha \sum_{s=1}^{S}\sum_{k=1}^{K} \psi_{sk}[n] + \sum_{s=1}^{S} \theta_m \left(P_s^{\max} - \sum_{k=1}^{K} p_{sk}[n]\right) \\ &\quad + \sum_{s=1}^{S}\sum_{k=1}^{K} \chi_{sk}[n]\left\{\omega_s R_{skm}[n] - \psi_{sk}[n] P_{sk}^{total}[n]\right\}. \end{aligned} \tag{32}$$

According to theorem 4.2.8 in [46], i.e., Fritz-John optimization conditions, we know that there exist $\alpha^*, \boldsymbol{\beta}^*, \boldsymbol{\theta}^*$ and $\boldsymbol{\chi}^*[n]$ and the following equations can be met.

$$\frac{\partial L}{\partial p_{sk}[n]} = 0, \quad \forall s, k, \tag{33}$$

$$\frac{\partial L}{\partial \psi_{mk}[n]} = \alpha^* - \chi_{mk}^*[n] P_{sk}^{total}[n] = 0, \quad \forall s, k, \tag{34}$$

$$\begin{aligned} \beta_{sk}^* \frac{\partial L}{\partial \beta_{sk}^*} &= \beta_{sk}^* \Bigg[p_{sk}[n] g_{skm} \\ &\quad + \left(1 - 2^{\frac{NR_m^{\min}}{B_0 N_{sm,act} K_m}}\right)\left(I_{mk} + \sigma^2\right)\Bigg] = 0, \\ &\quad \forall s, k, \end{aligned} \tag{35}$$

$$\theta_s^* \frac{\partial L}{\partial \theta_s^*} = \theta_s^* \left(P_s^{\max} - \sum_{k=1}^{K} p_{sk}[n]\right) = 0, \ \forall s, \tag{36}$$

$$\begin{aligned} \chi_{mk}^*[n] \frac{\partial L}{\partial \chi_{mk}^*[n]} &= \chi_{mk}^*[n]\left[\omega_s R_{skm}[n]\right. \\ &\quad \left. - \psi_{sk}[n] P_{sk}^{total}[n]\right] = 0, \quad \forall s, k, \end{aligned} \tag{37}$$

$$C1', C3, C4, C6, \tag{38}$$

$$\alpha^* \geq 0, \boldsymbol{\beta}^*, \boldsymbol{\theta}^*, \boldsymbol{\chi}^*[n] \geq \mathbf{0}. \tag{39}$$

Suppose $\alpha^* = 0, \forall p_{sk}[n] \in \mathbf{P}[n]$. Since $P_{sk}^{total}[n] > 0$ in (34), we have $\chi_{mk}^*[n] = 0$. Therefore, from equations (33), (35)-(37), we can obtain

$$\sum_{s \in \mathcal{I}(\mathbf{P}^*[n])} \beta_{sk}^* \nabla g_{sk}\left(\mathbf{P}^*[n]\right) = 0, \tag{40}$$

$$\sum_{s \in \mathcal{I}(\mathbf{P}^*[n])} \beta_{sk}^* > 0, \beta_{sk}^* \geq 0, \quad \forall s, k, \tag{41}$$

where

$$g_{sk}\left(\mathbf{P}^*[n]\right) = \left(2^{\frac{NR_m^{\min}}{B_0 N_{sm,act} K_m}}-1\right)\left(I_{mk}+\sigma^2\right)-p_{sk}^*[n]\, g_{skm},$$

$$\mathcal{I}\left(\mathbf{P}^*[n]\right) = \left\{ s|p_{sk}^*[n]\, g_{skm}+\left(1-2^{\frac{NR_m^{\min}}{B_0 N_{sm,act} K_m}}\right)\left(I_{sk}+\sigma^2\right)=0 \right\}.$$

According to the Slater condition, there exists $\mathbf{P}'$, satisfying

$$g_{sk}\left(\mathbf{P}'[n]\right) < 0, \quad \forall s,k. \tag{42}$$

Since $g_{sk}\left(\mathbf{P}^*[n]\right)$ is convex with respect to $\mathbf{P}^*[n]$, $\forall s \in \mathcal{I}\left(\mathbf{P}^*[n]\right)$, we have

$$\nabla g_{sk}\left(\mathbf{P}^*[n]\right)^T\left(\mathbf{P}'[n]-\mathbf{P}^*[n]\right) \le g_{sk}\left(\mathbf{P}'[n]\right)-g_{sk}\left(\mathbf{P}^*[n]\right) < 0. \tag{43}$$

Let $\mathbf{d}=\mathbf{P}'[n]-\mathbf{P}^*[n]$, from (41) and (43), we can obtain

$$\left(\sum_{s\in\mathcal{I}(\mathbf{P}^*[n])} \beta_{sk}^* \nabla g_{sk}\left(\mathbf{P}^*[n]\right)\right)^T \mathbf{d} < 0, \tag{44}$$

which is in contradiction with (40). Thus $\alpha^* > 0$.

Replace $\chi_{sk}^*[n]$ and β_{sk}^* with $\frac{\chi_{sk}^*[n]}{\alpha^*}$ and $\frac{\beta_{sk}^*}{\alpha^*}$, respectively. According (34) and (37), we can obtain (25). Given $\chi_{sk}[n]=\chi_{sk}^*[n]$ and $\psi_{sk}[n]=\psi_{sk}^*[n]$, (33), (35) and (36) are Karush-Kuhn-Tucker (KKT) conditions of problem (24). Therefore, for $\chi_{sk}[n]=\chi_{sk}^*[n]$ and $\psi_{sk}[n]=\psi_{sk}^*[n]$, $\mathbf{P}^*[n]$ is a solution of problem (24).

APPENDIX B
PROOF OF THEOREM 2

According to [41], we construct minorization function G in $\mathcal{P}\times\mathcal{P}$, satisfying

$$\begin{cases} U\left(\mathbf{P}[n]\right) \ge G(\mathbf{P}[n],\mathbf{Q}[n]), \forall \mathbf{P}[n],\mathbf{Q}[n]\in\mathcal{P}, \\ U\left(\mathbf{P}[n]\right) = G(\mathbf{P}[n],\mathbf{P}[n]), \forall \mathbf{P}[n]\in\mathcal{P}. \end{cases} \tag{45}$$

Therefore, $G(\cdot)$ is the lower bound of $U(\cdot)$ and is equal to $U(\cdot)$ at $\mathbf{Q}[n]$. According to the minorization algorithm, the iterations of $\mathbf{P}[n]$ are as follows:

$$\mathbf{P}^{(l+1)}[n] = \arg\max_{\mathbf{P}[n]\in\mathcal{P}} \left\{ G\left(\mathbf{P}[n],\mathbf{P}^{(l)}[n]\right)\right\}. \tag{46}$$

If and only if $\mathbf{P}^{(l)}[n] = \arg\max_{\mathbf{P}[n]\in\mathcal{P}} \left\{G\left(\mathbf{P}[n],\mathbf{P}^{(l)}[n]\right)\right\}$ or $\left\|\mathbf{P}^{(l+1)}-\mathbf{P}^{(l)}\right\| < \varepsilon$, the algorithm stops. It is easy to prove that $U\left(\mathbf{P}[n]\right)$ increases monotonically in each iteration, i.e.,

$$U\left(\mathbf{P}^{(l+1)}[n]\right) \overset{(a)}{\ge} G\left(\mathbf{P}^{(l+1)}[n],\mathbf{P}^{(l)}[n]\right) \overset{(b)}{\ge} G\left(\mathbf{P}^{(l)}[n],\mathbf{P}^{(l)}[n]\right) \overset{(c)}{=} U\left(\mathbf{P}^{(l)}[n]\right), \tag{47}$$

where (a) and (c) are obtained through (45) and (b) through (46). The main idea of CCCP algorithm is to change the convex part of $U\left(\mathbf{P}[n]\right)$, i.e., $-U_{cave2}\left(\mathbf{P}[n]\right)$, to be linear through iteration. According to [41], use Taylor approximation to build the minorization function G. Since $-U_{cave2}\left(\mathbf{P}[n]\right)$ is convex and differentiable, the following inequality is true.

$$-U_{\text{cave2}}\left(\mathbf{P}[n]\right) \ge -U_{\text{cave2}}\left(\mathbf{Q}[n]\right)-\left(\mathbf{P}[n]-\mathbf{Q}[n]\right)^T * \nabla U_{\text{cave2}}\left(\mathbf{Q}[n]\right), \quad \forall \mathbf{P}[n],\mathbf{Q}[n]\in\mathcal{P}. \tag{48}$$

Add $U_{cave1}\left(\mathbf{P}[n]\right)$ to both sides of this equation, and we obtain

$$\begin{aligned} U\left(\mathbf{P}[n]\right) &= U_{\text{cave1}}\left(\mathbf{P}[n]\right)-U_{\text{cave2}}\left(\mathbf{P}[n]\right) \\ &\ge U_{\text{cave1}}\left(\mathbf{P}[n]\right)-U_{\text{cave2}}\left(\mathbf{Q}[n]\right) \\ &\quad -\left(\mathbf{P}[n]-\mathbf{Q}[n]\right)^T * \nabla U_{\text{cave2}}\left(\mathbf{Q}[n]\right), \\ &\quad \forall \mathbf{P}[n],\mathbf{Q}[n]\in\mathcal{P}. \end{aligned} \tag{49}$$

Define the minorization function as

$$G(\mathbf{P}[n],\mathbf{Q}[n]) \triangleq U_{\text{cave1}}\left(\mathbf{P}[n]\right)-U_{\text{cave2}}\left(\mathbf{Q}[n]\right) -\left(\mathbf{P}[n]-\mathbf{Q}[n]\right)^T * \nabla U_{\text{cave2}}\left(\mathbf{Q}[n]\right), \quad \forall \mathbf{P}[n],\mathbf{Q}[n]\in\mathcal{P}. \tag{50}$$

According to (46), the following convex programming can be used to solve the problem (27):

$$\begin{aligned} \mathbf{P}^{(l+1)}[n] &= \arg\max_{\mathbf{P}[n]\in\mathcal{P}} \theta \left\{ U_{\text{cave1}}\left(\mathbf{P}[n]\right)-U_{\text{cave2}}\left(\mathbf{P}^{(l)}[n]\right) \right. \\ &\quad \left. -\left(\mathbf{P}[n]-\mathbf{P}^{(l)}[n]\right)^T * \nabla U_{\text{cave2}}\left(\mathbf{P}^{(l)}[n]\right)\right\} \\ &= \arg\max_{\mathbf{P}[n]\in\mathcal{P}} \left\{ U_{\text{cave1}}\left(\mathbf{P}[n]\right)-\mathbf{P}^{(T)}[n] * \nabla U_{\text{cave2}}\left(\mathbf{P}^{(l)}[n]\right)\right\}. \end{aligned} \tag{51}$$

Therefore, the problem (27) can be solved through (28).

REFERENCES

[1] P. Gandotra, R. K. Jha, and S. Jain, "Green communication in next generation cellular networks: A survey," *IEEE Access*, vol. 5, pp. 11727–11758, Jun. 2017.
[2] G. Wu, C. Yang, S. Li, and G. Y. Li, "Recent advances in energy-efficient networks and their application in 5G systems," *IEEE Wireless Commun.*, vol. 22, no. 2, pp. 145–151, Apr. 2015.
[3] C. Yang, J. Li, A. Anpalagan, and M. Guizani, "Joint power coordination for spectral-and-energy efficiency in heterogeneous small cell networks: A bargaining game-theoretic perspective," *IEEE Trans. Wireless Commun.*, vol. 15, no. 2, pp. 1364–1376, Feb. 2016.
[4] V. W. Wong, R. Schober, D. W. K. Ng, and L.-C. Wang, *Key Technologies for 5G Wireless Systems*. Cambridge, U.K.: Cambridge Univ. Press, 2017.
[5] H. Celebi and I. Guvenc, "Load analysis and sleep mode optimization for energy-efficient 5G small cell networks," in *Proc. IEEE Int. Conf. Commun. Workshops (ICC Workshops)*, Paris, France, May 2017, pp. 1159–1164.
[6] R. Tao, W. Liu, X. Chu, and J. Zhang, "An energy saving small cell sleeping mechanism with cell range expansion in heterogeneous networks," *IEEE Trans. Wireless Commun.*, vol. 18, no. 5, pp. 2451–2463, May 2019.

[7] A. Dataesatu, P. Boonsrimuang, K. Mori, and P. Boonsrimuang, "Energy efficiency enhancement in 5G heterogeneous cellular networks using system throughput based sleep control scheme," in *Proc. 22nd Int. Conf. Adv. Commun. Technol. (ICACT)*, PyeongChang, South Korea, Feb. 2020, pp. 549–553.

[8] H. B. Ren, W. Y. Zhou, M. Zhao, and J. K. Zhu, "Energy-efficient resource allocation for OFDMA networks with sleep mode," *Electron. Lett.*, vol. 49, no. 2, pp. 111–113, Jan. 2013.

[9] S. Mishra and C. S. R. Murthy, "Increasing energy efficiency via transmit power spreading in dense femto cell networks," *IEEE Syst. J.*, vol. 12, no. 1, pp. 971–980, Mar. 2018.

[10] S. Xu, R. Li, and Q. Yang, "Improved genetic algorithm based intelligent resource allocation in 5G ultra dense networks," in *Proc. IEEE Wireless Commun. Netw. Conf. (WCNC)*, Barcelona, Spain, Apr. 2018, pp. 1–6.

[11] I. AlQerm and B. Shihada, "Sophisticated online learning scheme for green resource allocation in 5G heterogeneous cloud radio access networks," *IEEE Trans. Mobile Comput.*, vol. 17, no. 10, pp. 2423–2437, Oct. 2018.

[12] R. Yin, Y. Zhang, and G. Y. Li, "Energy efficiency in LTE-U based small cell systems," *IEEE Access*, vol. 6, pp. 64050–64062, Oct. 2018.

[13] R. Yin, Y. Zhang, F. Dong, A. Wang, and C. Yuen, "Energy efficiency optimization in LTE-U based small cell networks," *IEEE Trans. Veh. Technol.*, vol. 68, no. 2, pp. 1963–1967, Feb. 2019.

[14] H. Zhang, H. Liu, J. Cheng, and V. C. M. Leung, "Downlink energy efficiency of power allocation and wireless backhaul bandwidth allocation in heterogeneous small cell networks," *IEEE Trans. Commun.*, vol. 66, no. 4, pp. 1705–1716, Apr. 2018.

[15] J. Zheng, L. Gao, H. Zhang, D. Zhu, H. Wang, Q. Gao, and V. C. M. Leung, "Joint energy management and interference coordination with max-min fairness in ultra-dense HetNets," *IEEE Access*, vol. 6, pp. 32588–32600, May 2018.

[16] L. D. Nguyen, H. D. Tuan, T. Q. Duong, O. A. Dobre, and H. V. Poor, "Downlink beamforming for energy-efficient heterogeneous networks with massive MIMO and small cells," *IEEE Trans. Wireless Commun.*, vol. 17, no. 5, pp. 3386–3400, May 2018.

[17] D. W. K. Ng, E. S. Lo, and R. Schober, "Energy-efficient resource allocation in multi-cell OFDMA systems with limited backhaul capacity," *IEEE Trans. Wireless Commun.*, vol. 11, no. 10, pp. 3618–3631, Oct. 2012.

[18] C. K. Ho, D. Yuan, L. Lei, and S. Sun, "Power and load coupling in cellular networks for energy optimization," *IEEE Trans. Wireless Commun.*, vol. 14, no. 1, pp. 509–519, Jan. 2015.

[19] J. Chen, H. Zhuang, and Z. Luo, "Energy optimization in dense OFDM networks," *IEEE Commun. Lett.*, vol. 20, no. 1, pp. 189–192, Jan. 2016.

[20] L. Lei, D. Yuan, C. K. Ho, and S. Sun, "Optimal cell clustering and activation for energy saving in load-coupled wireless networks," *IEEE Trans. Wireless Commun.*, vol. 14, no. 11, pp. 6150–6163, Nov. 2015.

[21] N.-T. Le, L.-N. Tran, Q.-D. Vu, and D. Jayalath, "Energy-efficient resource allocation for OFDMA heterogeneous networks," *IEEE Trans. Commun.*, vol. 67, no. 10, pp. 7043–7057, Oct. 2019.

[22] S. Wu, Z. Zeng, and H. Xia, "Load-aware energy efficiency optimization in dense small cell networks," *IEEE Commun. Lett.*, vol. 21, no. 2, pp. 366–369, Feb. 2017.

[23] S. Buzzi, C.-L. I, T. E. Klein, H. V. Poor, C. Yang, and A. Zappone, "A survey of energy-efficient techniques for 5G networks and challenges ahead," *IEEE J. Sel. Areas Commun.*, vol. 34, no. 4, pp. 697–709, Apr. 2016.

[24] A. A. Salem, S. El-Rabaie, and M. Shokair, "Energy efficient ultra-dense networks (UDNs) based on joint optimisation evolutionary algorithm," *IET Commun.*, vol. 13, no. 1, pp. 99–107, Jan. 2019.

[25] W. Ur Rehman, A. Hussain, and M. M. Butt, "Joint user association and BS switching scheme for green heterogeneous cellular network," in *Proc. IEEE Globecom Workshops (GC Wkshps)*, Abu Dhabi, United Arab Emirates, Dec. 2018, pp. 1–6.

[26] W. Lu, S. Fang, S. Hu, X. Liu, B. Li, Z. Na, and Y. Gong, "Energy efficiency optimization for OFDM based 5G wireless networks with simultaneous wireless information and power transfer," *IEEE Access*, vol. 6, pp. 75937–75946, Nov. 2018.

[27] J. Joung, C. K. Ho, K. Adachi, and S. Sun, "A survey on power-amplifier-centric techniques for spectrum- and energy-efficient wireless communications," *IEEE Commun. Surveys Tuts.*, vol. 17, no. 1, pp. 315–333, 1st Quart., 2015.

[28] A. N. Al-Quzweeni, A. Q. Lawey, T. E. H. Elgorashi, and J. M. H. Elmirghani, "Optimized energy aware 5G network function virtualization," *IEEE Access*, vol. 7, pp. 44939–44958, Mar. 2019.

[29] Z. Xu, X. Zhang, S. Yu, and J. Zhang, "Energy-efficient virtual network function placement in telecom networks," in *Proc. IEEE Int. Conf. Commun. (ICC)*, Kansas City, MO, USA, May 2018, pp. 1–7.

[30] Y. Zhang, Y. Xu, Y. Sun, Q. Wu, and K. Yao, "Energy efficiency of small cell networks: Metrics, methods and market," *IEEE Access*, vol. 5, pp. 5965–5971, Apr. 2017.

[31] S. Wu, R. Yin, N. Dong, and X. Liu, "Heterogeneity-based energy-efficient transmission in dense small cell networks," in *Proc. IEEE Wireless Commun. Netw. Conf. (WCNC)*, Seoul, South Korea, May 2020, pp. 1–6.

[32] W. Dinkelbach, "On nonlinear fractional programming," *Manage. Sci.*, vol. 13, no. 7, pp. 492–498, Mar. 1967.

[33] E. Pateromichelakis, M. Shariat, A. Quddus, M. Dianati, and R. Tafazolli, "Dynamic clustering framework for multi-cell scheduling in dense small cell networks," *IEEE Commun. Lett.*, vol. 17, no. 9, pp. 1802–1805, Sep. 2013.

[34] W. Jing, Z. Lu, H. Zhang, Z. Zhang, J. Zhao, and X. Wen, "Energy-saving resource allocation scheme with QoS provisioning in OFDMA femtocell networks," in *Proc. IEEE Int. Conf. Commun. Workshops (ICC)*, Sydney, NSW, Australia, Jun. 2014, pp. 912–917.

[35] G. Auer, V. Giannini, C. Desset, I. Godor, P. Skillermark, M. Olsson, M. Imran, D. Sabella, M. Gonzalez, O. Blume, and A. Fehske, "How much energy is needed to run a wireless network?" *IEEE Wireless Commun.*, vol. 18, no. 5, pp. 40–49, Oct. 2011.

[36] C. He, B. Sheng, P. Zhu, and X. You, "Energy efficiency and spectral efficiency tradeoff in downlink distributed antenna systems," *IEEE Wireless Commun. Lett.*, vol. 1, no. 3, pp. 153–156, Jun. 2012.

[37] Q. Ye, B. Rong, Y. Chen, M. Al-Shalash, C. Caramanis, and J. G. Andrews, "User association for load balancing in heterogeneous cellular networks," *IEEE Trans. Wireless Commun.*, vol. 12, no. 6, pp. 2706–2716, Jun. 2013.

[38] J. Kim, I. Bang, D. K. Sung, Y. Yi, and B.-H. Kim, "Design of a multi-variable QoE function based on the remaining battery energy," in *Proc. IEEE 26th Annu. Int. Symp. Pers., Indoor, Mobile Radio Commun. (PIMRC)*, Hong Kong, Aug. 2015, pp. 976–980.

[39] S. Wu, F. Liu, Z. Zeng, and H. Xia, "Cooperative sleep and power allocation for energy saving in dense small cell networks," *IEEE Access*, vol. 4, pp. 6993–7004, Oct. 2016.

[40] Y. Jong. (May 2012). *An Efficient Global Optimization Algorithm for Nonlinear Sum-of-Ratios Problem*. [Online]. Available: http://www.optimization-online.org/DB_FILE/2012/08/3586.pdf

[41] G. R. Lanckriet and B. K. Sriperumbudur, "On the convergence of the concave-convex procedure," in *Proc. Adv. Neural Inf. Process. Syst.*, 2009, pp. 1759–1767.

[42] *Further Advancements for E-Utra Physical Layer Aspects*, document 3GPP TR 36.814, 2010.

[43] R. Jain, D. M. Chiu, and W. Hawe, *A Quantitative Measure of Fairness and Discrimination for Resource Allocation in Shared Systems, Digital Equipment Corporation*, document DEC-TR-301, 1984.

[44] N. Zhao, F. Cheng, F. R. Yu, J. Tang, Y. Chen, G. Gui, and H. Sari, "Caching UAV assisted secure transmission in hyper-dense networks based on interference alignment," *IEEE Trans. Commun.*, vol. 66, no. 5, pp. 2281–2294, May 2018.

[45] N. Zhao, X. Liu, F. R. Yu, M. Li, and V. C. M. Leung, "Communications, caching, and computing oriented small cell networks with interference alignment," *IEEE Commun. Mag.*, vol. 54, no. 9, pp. 29–35, Sep. 2016.

[46] M. S. Bazaraa, H. D. Sherali, and C. M. Shetty, *Nonlinear Programming: Theory Algorithms*. Hoboken, NJ, USA: Wiley, 2013.

SHIE WU received the B.S. degree in electronic and information engineering from Yantai University, Yantai, China, in 2010, and the M.S. degree in electronic and communication engineering and the Ph.D. degree in information and communication engineering from the Beijing University of Posts and Telecommunication (BUPT), Beijing, China, in 2013 and 2017, respectively.

She is currently a Lecturer with the School of Opto-Electronic Information Science and Technology, Yantai University. Her current research interests include radio resource management, energy efficiency, and cooperative communications in dense small cell networks and mobile edge computing systems.

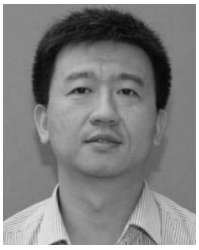

RUI YIN (Senior Member, IEEE) received the B.S. degree in computer engineering from Yanbian University, China, in 2001, the M.S. degree in computer engineering from KwaZulu-Natal University, Durban, South Africa, in 2006, and the Ph.D. degree in information and electronic engineering from Zhejiang University, China, in 2011.

From March 2011 to June 2013, he was a Research Fellow with the Department of Information and Electronic Engineering, Zhejiang University. He is currently a Professor with the School of Information and Electrical Engineering, Zhejiang University City College, China, and a joint Honorary Research Fellow with the School of Electrical, Electronic, and Computer Engineering, University of KwaZulu-Natal. His research interests include radio resource management in LTE unlicensed, millimeter wave cellular wireless networks, HetNet, cooperative communications, massive MIMO, optimization theory, game theory, and information theory. He regularly serves on the Technical Program Committee (TPC) boards of prominent IEEE conferences, such as ICC, GLOBECOM, and PIMRC, and chairs some of their technical sessions.

CELIMUGE WU (Senior Member, IEEE) received the M.E. degree from the Beijing Institute of Technology, China, in 2006, and the Ph.D. degree from The University of Electro-Communications, Japan, in 2010.

He is currently an Associate Professor with the Graduate School of Informatics and Engineering, The University of Electro-Communications. His current research interests include vehicular networks, sensor networks, intelligent transport systems, the IoT, and mobile cloud computing. He is/has been the TPC Co-Chair of Wireless Days 2019, ICT-DM 2019, and ICT-DM 2018. He is also the Chair of IEEE TCBD Special Interest Group on Big Data with Computational Intelligence. He is/has been serving as an Associate Editor for IEEE ACCESS, the *IEICE Transactions on Communications*, the *International Journal of Distributed Sensor Networks*, and *Sensors* (MDPI), and a Guest Editor for the IEEE TRANSACTIONS ON EMERGING TOPICS IN COMPUTATIONAL INTELLIGENCE, the *IEEE Computational Intelligence Magazine*, and *ACM/Springer MONET*.